JOURNAL OF SOLID STATE CHEMISTRY 103, 25–29 (1993)

The ^{57}Fe Mössbauer Isomer Shift in Microdoped Monoxides

M. G. SMITH AND J. B. GOODENOUGH

Center for Materials Science and Engineering, ETC 9.104, The University of Texas at Austin, Austin, Texas 78712

Received March 24, 1992; in revised form July 16, 1992; accepted July 17, 1992

Comparison of the room-temperature Mössbauer isomer shifts (I.S.) of the Fe^{2+} and Fe^{3+} daughter states of the ^{57}Co-microdoped monoxides MO with M = Mg, Ca, Mn, Co, Ni, or Cu have been correlated with high-pressure data for M = Co and α-Fe_2O_3. Any empirical relationship relating the I.S. to the mean iron valence $\langle m \rangle$ relative to 10^{-8} sec that is applicable to iron oxides with a large iron-atom concentration needs to modified for microdoped samples where the Co–O bond length does not have its normal equilibrium value and the counter cations introduce an inductive effect. A nearly linear dependence of the I.S. on bond length is found for bond lengths near their normal value: d(I.S.)/d(Co–O) $\approx$ 1.08 (mm/sec)/Å for the $^{57}Fe^{2+}$ daughter and 0.83 (mm/sec)/Å for the $^{57}Fe^{3+}$ daughter. Covalent Fe–O σ-bonding is increased—and hence, the I.S. is decreased—either by bending of the 180° Fe–O–Fe bond from 180° toward 90° or by introducing more electropositive counter cations M in the 180° Fe–O–M bonds. Application to ^{57}Co microdoped copper oxides indicates that the $Co^{3+/2+}$ redox couple tends to lie in the narrow energy range between the $Cu^{2+/+}$ and $Cu^{3+/2+}$ redox couples.

Introduction

An empirical relationship for the room-temperature isomer shift (I.S.) with respect to α-Fe of high-spin ^{57}Fe in octahedral (VI) and tetrahedral (IV) oxygen coordination in an oxide has been proposed (*1*) for iron oxides containing a high concentration of iron atoms:

$$\text{I.S.(VI)} \approx (2.85\text{–}0.85\langle m \rangle \pm 0.1) \text{ mm/sec}$$

$$\text{I.S.(IV)} \approx (2.6\text{–}0.8\langle m \rangle \pm 0.1) \text{ mm/sec},$$

where $2 \leq \langle m \rangle \leq 3$ is the mean formal valence of the iron on a time scale $\tau > 10^{-8}$ sec.

Whereas the monoxides MO with M = Mg, Ca, Mn, Co, and Ni crystallize in the rocksalt structure, CuO exhibits a cooperative Jahn–Teller distortion to monoclinic (*2*) in which each Cu atom is coordinated to four oxygen at a Cu–O bond length of 1.95 Å and two oxygen at 2.78 Å. Shah and Gupta (*3*) have observed a ^{57}Fe room-temperature I.S. = 0.359(4) mm/sec in CuO with 0.5 at.% Fe substituted for Cu. In accordance with Eq. (1) this value is typical for Fe^{3+} in sixfold coordination; it appears to be a little too high for Fe^{3+} in fourfold coordination. Since the $Fe^{3+/2+}$ redox level is known to be at a higher energy than the $Cu^{3+/2+}$ redox couple in oxides (*4*), the electron-transfer reaction

$$Fe^{2+} + Cu^{2+} \rightarrow Fe^{3+} + Cu^{+} \qquad (2)$$

stabilizes Fe^{3+} in CuO : Fe, so a measured I.S. typical for Fe^{3+} brings no particular surprise.

On the other hand, Mössbauer emission

0022-4596/93 $5.00

studies (*5–8*) of CuO(^{57}Co) show several components of varying intensities. The principal component has a reported room-temperature I.S. of $0.68 \leq$ I.S. ≤ 0.75 mm/sec (we disregard an early report, *5*, of 0.44 mm/sec). A satellite component has an isomer shift in the range $0.2 \leq$ I.S. ≤ 0.31 mm/sec. Impurity phases are reported with isomer shifts of 0.95 mm/sec (Ref. *5*) and 0.31(8) mm/sec (Ref. *8*). The principal component is due to a $^{57}Fe^{2+}$ daughter, and the satellite at 0.2–0.31 mm/sec is from a $^{57}Fe^{3+}$ daughter ion. However, an I.S. = 0.68(2) mm/sec lies midway between the values predicted for Fe^{3+} and Fe^{2+} from Eq. (1), which raises a question about the general applicability of Eq. (1). Moreover, the results have led to a disagreement in the literature (*3, 6–8*) as to whether Co is present as Co^{2+} or Co^{3+} in microdoped CuO(^{57}Co).

Discussion

The Mössbauer isomer shift between the source A and an absorber B is proportional to the difference in *s*-electron density at the nucleus,

$$\text{I.S.} \sim (|^s\psi_A(0)|^2 - |^s\psi_B(0)|^2). \qquad (3)$$

Whereas the reference species, metallic α-Fe, contains 4*s* electrons, Fe cations in an "ionic compound see a 4*s* contribution only by virtue of electron back transfer to the Fe-4*s* orbitals via covalent mixing. Although covalent electron back transfer to empty 3*d* orbitals increases the screening of the core *s* electrons from the nuclear charge, the resulting decrease in $|^s\psi(0)|^2$ from this cause is weaker than the increase from the 4*s* contribution (*9*). It follows qualitatively that the weaker the covalent bonding, the larger the I.S. with respect to α-Fe. Consequently, an Fe^{2+} ion has a larger I.S. than an Fe^{3+} ion, and a high-spin configuration has a larger I.S. than a low-spin configuration. It also follows that the I.S. for a given formal valence and anion (*X*) coordination should increase with the mean Fe-*X* bond length. In addition, bending of an Fe–*X*–Fe bond from 180° toward 90° would increase the covalent character of the σ-bonding; bending reduces the competition of the two cations for the same p_σ orbital. Moreover, if an iron atom has unlike near-neighbor cations, then the character of the *M*–*X* bonding in a 180° Fe–X–*M* bond will influence the strength of the covalent component to the Fe–*X* bonding via the inductive effect. Equation (1) is therefore applicable only where the mean Fe–O bond length approaches its atmospheric-pressure equilibrium value and any inductive effect does not alter the covalent component of the Fe–*X* bond significantly from what is found in an Fe–*X*–Fe bond. In a microdoped sample, both the mean Fe–O bond length and the inductive effect may deviate significantly from their values in iron oxides; in this case it is necessary to recognize the limitation of Eq. (*1*), which is based on iron oxides having a high iron concentration.

In order to demonstrate the influence on I.S. of both a changing Fe–O bond length and the inductive effect, we plot in Fig. 1 the observed (*6–8, 10–16*) room-temperature isomer shifts for the $^{57}Fe^{2+}$ and $^{57}Fe^{3+}$ components of the microdoped monoxides *M*O(^{57}Co) versus the room-temperature *M*–O bond length in the rocksalt structures (*M* = Mg, Ca, Mn, Co, Ni) and versus the short Cu–O bond length in CuO. At room temperature, only NiO is antiferromagnetic with a small exchange-strictive distortion to rhombohedral symmetry, and this distortion does not influence the I.S. We do not include the I.S. for the $^{57}Fe^{2+}$ and $^{57}Fe^{3+}$ components of $Fe_{1-\delta}O$ determined from Mössbauer absorption spectroscopy (*17–20*) for these reasons: (1) difficulties in fitting the data have resulted in a wide spread of reported values, (2) electron transfer between the octahedral-site Fe^{3+} and Fe^{2+} ions, although slow relative to the 10^{-8} sec time scale of the Mössbauer experiment, does

reduce the Fe^{2+} and enhances the Fe^{3+} values, and (3) there is no good measure of the tetrahedral-site bond length. The isomer shifts of the principal component of the room-temperature ^{57}Fe Mössbauer emission spectra from $MO(^{57}Co)$ with M = Mg, Ca, Mn, Co, or Ni are found to be in good agreement with Eq. (1) for I.S. (VI) and $\langle m \rangle = 2$, whereas the observed I.S. of the principal component for $CuO(^{57}Co)$ would seem to imply, according to Eq. (1), an $\langle m \rangle \approx 2.5$.

In order to obtain a measure of the influence of the bond-length change alone on I.S., we turn again to published data; high-pressure Mössbauer (*16, 21*) and X-ray diffraction (*22, 23*) data are available for CoO and α-Fe_2O_3. In Fig. 1 we plot the dependence of the I.S. of the $^{57}Fe^{2+}$ room-temperature daughter of $CoO(^{57}Co)$ versus the Co–O bond length as calculated from the independent high-pressure measurements. We calculate a slope d(I.S.)/d(Co–O) = +1.08 (mm/sec)/Å and plot a dashed line with this slope through the $CoO(^{57}Co)$ data in Fig. 1. The corundum structure of α-Fe_2O_3 contains Fe in distorted octahedral sites; pairs of Fe^{3+} ions share common octahedral faces, and the electrostatic repulsive force between them repels each iron toward the octahedral-site face opposite the one that is shared. Consequently, two Fe–O bond lengths (1.96 and 2.09 Å) are found at room temperature and atmospheric pressure. In Fig. 1 we plot the dependence of the I.S. for $^{57}Fe^{3+}$ on the shorter of the Fe–O bond lengths as calculated from the independent high-pressure measurements. The α-Fe_2O_3 structure is stable to 90 GPa (*24*); we calculate for the shorter Fe–O bond length a slope d(I.S.)/d(Fe–O) = +1.37 (mm/sec)/Å for pressures $P < 1$ GPa and +0.83 (mm/sec)/Å for pressures $P > 1$ GPa. The solid line through the data of α-Fe_2O_3 in Fig. 1 has the high-pressure slope.

Extrapolation of the dashed line in Fig. 1 gives an I.S.(VI) = 0.88 mm/sec for an M–O

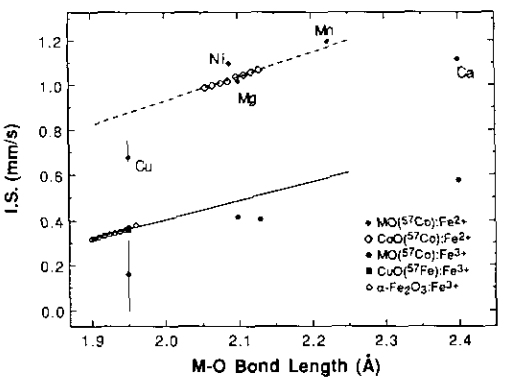

FIG. 1. Room-temperature ^{57}Fe isomer shift (I.S.) versus metal (M)–oxygen bond length in $MO(^{57}Co)$ (M = Mg, Ca, Mn, Co, Ni, Cu) and α-Fe_2O_3. Isomer shifts have been converted to absorber data and are with respect to α-Fe. Vertical lines correspond to the reported ranges of I.S. of the principal $^{57}Fe^{2+}$ and daughter $^{57}Fe^{3+}$ components of CuO (^{57}Co). The dashed and solid lines through the $CoO(^{57}Co)$ and α-Fe_2O_3 data, respectively, are calculated from the pressure dependence of the M–O bond length and I.S. (see text).

bond length of 1.95 Å, which remains larger than the I.S. = 0.68 ≤ I.S. ≤ 0.75 mm/sec observed for $CuO(^{57}Co)$. However, bending of the Fe–O–Cu bond from 180° to near 100° should enhance the covalent bonding to lower the predicted I.S. from 0.88 mm/sec. Moreover, according to Eq. (1) reduction from sixfold to fourfold coordination may be expected to reduce the I.S. by about 0.1 mm/sec, which corresponds to an expected I.S.(IV) < 0.78 mm/sec. We believe the reduced I.S. for $^{57}Fe^{2+}$ in $CuO(^{57}Co)$ reflects an enhanced covalent contribution to the Fe–O bond due to not only a shorter Fe–O bond length, but also to a reduction of the Fe–O–Cu bond angle from 180° to near 100°, which eliminates competition for the same O : 2p orbital by the bridged cations. Moreover, there is also an inductive effect in microdoped samples. Comparison of the $^{57}Fe^{2+}$ daughter I.S. for $MgO(^{57}Co)$ and $CaO(^{57}Co)$ suggests that the inductive effect compensates for much of the size effect in $CaO(^{57}Co)$. Although a strongly cova-

lent component in the Cu–O bond might be expected to reduce the covalent component at an Fe atom sharing a common bridging oxygen, this effect is reduced by a bond angle of 100° since the two ions do not compete for the same O : 2*p* orbital at a 90° bond angle.

The $Co^{3+/2+}$ couple lies close to the $Cu^{2+/+}$ couple in oxides, and it is not possible from semiempirical considerations to predict unambiguosly whether the charge-transfer reaction,

$$Cu^{2+} + Co^{2+} \rightarrow Cu^{+} + Co^{3+}, \quad (4)$$

is biased to the left or to the right in any given copper oxide. The observation of a principal $^{57}Fe^{2+}$ daughter component in the Mössbauer spectrum of CuO(^{57}Co) shows that the equilibrium reaction (4) is biased to the left and also that the lifetime of the $^{57}Fe^{2+}$ daughter state is $\tau > 10^{-8}$ sec for the electron-transfer reaction (2) after electron capture by the $^{57}Co^{2+}$ nucleus. The observation of a satellite component with an I.S. = 0.2(2) mm/sec implies the presence of another electron-transfer mechanism in the absence of a competitively fast electron transfer in reaction (2). In CoO(^{57}Co) and NiO(^{57}Co), cation vacancies create Co^{3+} and Ni^{3+} species, and the $^{57}Fe^{3+}$ satellites arise from the electron-transfer reactions

$$Fe^{2+} + M^{3+} \rightarrow Fe^{3+} + M^{2+} \quad (M = \text{Co or Ni}). \quad (5)$$

The $^{57}Fe^{3+}$ daughter satellites are stronger for cation-deficient MO(^{57}Co) with M = Co or Ni than is found for CuO(^{57}Co); this observation indicates that CuO is more nearly stoichiometric.

The ambiguity fo the directional bias of reaction (4) is highlighted by a comparison of the Mössbauer data for CuO and the high-temperature superconductor $YBa_2Cu_3O_{6+y}$ microdoped with ^{57}Co. Whereas CuO(^{57}Co) exhibits a $^{57}Fe^{2+}$ daughter and a $^{57}Fe^{3+}$ satellite, $YBa_2Cu_3O_{6+y}$(^{57}Co) shows no evidence for $^{57}Fe^{2+}$; it gives isomer shifts of 0.00 and 0.30 mm/sec for the ^{57}Fe daughters in, respectively, the Cu(1) chains and Cu(2) planes (*24*, *25*). These latter isomer shifts correspond to intermediate-spin and high-spin $^{57}Fe^{3+}$ daughter states, respectively. This result shows that *p*-type doping of the superconductive oxides has transformed reaction (4) to

$$p + Co^{2+} \rightarrow Co^{3+}, \quad (6)$$

where p is an itinerant-electron hole in the $(x^2 - y^2)$ band of a $(CuO_2)^{(2-p)-}$ sheet or $(z^2 - y^2)$ band of a $(CuO_2)^{(2-p)-}$ chain of the $YBa_2Cu_3O_{6+y}$ phase. It would appear that the $Co^{3+/2+}$ couple falls between the $Cu^{2+/+}$ and $Cu^{3+/2+}$ redox couples in oxides.

Conclusions

The above considerations lead to the following conclusions:

(1) The empirical equation (1) is applicable to iron oxides with a large iron-atom concentration, but it needs to be modified in microdoped samples where there is a non-equilibrium Fe–O bond length and/or an important inductive effect.

(2) The I.S. varies essentially linearly with bond length for bond lengths near their normal values:

d(I.S.)/d(Co–O) ≈ 1.08 (mm/sec)/Å for a $^{57}Fe^{2+}$ daughter

d(I.S.)/d(Co–O) ≈ 0.83 (mm/sec)/Å for a $^{57}Fe^{3+}$ daughter.

(3) The I.S. is decreased from its value for 180° M–O–M interactions by (a) reduction of the bond angle toward 90° and (b) introduction of a strongly electropositive counter cation M' in 180° M–O–M' bonds.

(4) The $Co^{3+/2+}$ redox couple tends to lie in the samll energy gap between the $Cu^{2+/+}$ and $Cu^{3+/2+}$ redox couples in copper oxides.

Acknowledgments

We thank the NSF, the Texas Advanced Research Program, and the R. A. Welch Foundation, Houston, Texas, for financial support.

References

1. C. Gleitzer and J. B. Goodenough, *Structure Bonding* **61,** 1 (1985).
2. S. Åsbrink and L. J. Norrby, *Acta Crystallogr.* **26,** 8 (1970).
3. P. Shah and A. Gupta, *Phys. Rev. B* **45,** 483 (1992).
4. J. B. Goodenough, *Progr. Solid State Chem.* **5,** 145 (1971).
5. S. S. Bhandari, J. S. Solanki, and J. Verma, *in* "Proc., Nuclear Physics and Solid State Physics Symposium," Vol. **18C,** p. 551 (1975).
6. Ch. Niedermayer, A. Golnik, E. Recknagel, M. Rossmanith, A. Wiedenger, X. S. Chang, A. Kleinhammes, N. Rosov, J. Saylor, R. Schuhmann, L. Takacs, A. Teh, G. Zhang, C. Hohenemser, and J. I. Budnick, *Phys. Rev. B* **38,** 2836 (1989).
7. A. Barcs, L. Bottyan, D. L. Nagy, N. S. Ovanesyan, and H. Spiering, *Hyperfine Interact.* **50,** 599 (1990).
8. M. G. Smith, R. D. Taylor, M. P. Pasternak, and H. Oesterreicher, *Phys. Rev. B* **42,** 2188 (1990).
9. H. Simanek and Z. Sroubek, *Phys. Rev.* **163,** 275 (1967).
10. J. D. Siegwarth, *Phys. Rev.* **155,** 285 (1967).
11. H. N. Ok and J. G. Mullen, *Phys. Rev.* **168,** 550 (1968); **168,** 563 (1968).
12. T. Harami, J. Loock, E. Huenges, J. Fontcuberta, X. Obradors, J. Tejada, and F. Parak, *J. Phys. Chem. Solids* **45,** 181 (1984).
13. J. Chappert, R. B. Frankel, A. Misetich, and N. A. Blum, *Phys. Rev.* **179,** 578 (1969).
14. J. R. Regnard, *Solid State Commun.* **12,** 207 (1973).
15. C. Song and J. G. Mullen, *Phys. Rev. B* **14,** 2761 (1976).
16. C. J. Coston, R. Ingalls, H. G. Drickamer, *Phys. Rev.* **2,** 409 (1966).
17. N. N. Greenwood and A. T. Howe, *J. Chem. Soc. Dalton Trans.* **122,** 110 (1972).
18. D. A. Hope, A. K. Cheetham, and G. J. Long, *Inorg. Chem.* **21,** 2804 (1982).
19. C. Gohy, A. Gerard, and F. Grandjean, *Phys. Status Solidi A* **74,** 583 (1982).
20. A. Pattek-Janczyk, B. Sepiol, J. C. Grenier, and L. Fournes, *Mater. Res. Bull.* **21,** 1083 (1986).
21. Y. Syono, A. Ito, S. Morimoto, T. Suzuki, T. Yagi, and S. Akimoto, *Solid State Commun.* **50,** 97 (1984).
22. R. L. Clendenen and H. G. Drickamer, *J. Chem. Phys.* **44,** 4223 (1966).
23. G. K. Lewis, Jr., and H. G. Drickamer, *J. Chem. Phys.* **45,** 224 (1966).
24. Z. Hommany, A. Nath, Y. Wei, and T. Jing, *Physica C* **174,** 223 (1991).
25. M. G. Smith, J. B. Goodenough, A. Manthiram, R. D. Taylor, and H. Oesterreicher, *J. Solid State Chem.* **99,** 140 (1992).